Source signature deconvolution of marine seismic data using deterministic modeling of the bubble signature

Leighton M. Watson, Joseph Jennings, and Shuki Ronen

ABSTRACT

Seismic airguns are not impulsive sources and hence marine seismic data must be designatured before interpretation. We demonstrate how deterministic modeling of the airgun signature can be used to designature field data. A heuristic approach is used to generalize the single airgun model to describe the signature of a small array of closely spaced guns where the bubbles from the different guns coalesce. The simulated signatures are used to designature data from a near-surface survey around a production rig. The results compare favorably to prediction-error filtering and the importance of using the correct source signature is illustrated.

INTRODUCTION

The data recorded in a seismic survey are the convolution of the source signature, wave propagation and the reflectivity. Estimating the reflectivity, or equivalently the velocity and density structure of the subsurface, is important for geological interpretation. In this paper, we discuss how marine seismic data can be designatured using deterministic modeling of the airgun signature.

Seismic airguns are the main source used in marine seismic surveys. An airgun functions by discharging highly pressurized air into the water, forming a bubble that expands and contracts. When the airgun discharges it produces a source signature with an initial peak due to the rapid expansion of the bubble and subsequent oscillations associated with the dynamics of the bubble expansion and collapse (Figure 1). Tuned airgun arrays have been used to minimize the bubble oscillations and make signature more impulsive (e.g., Dragoset, 2000), thereby simplifying the problem of source deconvolution. However, the signature of the airgun array can often still be seen in the data, especially for smaller arrays which cannot be tuned as well.

There are several methods for source designaturing. Statistical methods such as prediction-error filtering (PEF) are commonly used in the industry (Yilmaz, 2011). PEF attempts to solve the blind-deconvolution in which the spectrum of the signature is estimated and the deconvolution of the source signature are performed at the same time. Alternatively, the signature can be measured directly from near-field hydrophones and deconvolved from the data (Ziolkowski et al., 1981, 1984; Ziolkowski,

1991; Landrø et al., 1991; Landrø and Sollie, 1992; Laws et al., 1998; Kryvohuz and Campman, 2016) although there are some issues with the reliability of the near-field hydrophones and propagation of high frequency noise from the near-field to the far-field. Finally, physics-based modeling of the airgun-bubble dynamics can be used to estimate the source signature (Ziolkowski, 1970; Li et al., 2010; de Graaf et al., 2014; Watson et al., 2016). Commercial software packages like *Nucleus*®and *Gundalf*®use a combination of numerical modeling and measured signatures of individual airguns to determine the signature for an array of airguns.

Here, we examine how physics-based modeling of the airgun dynamics can be used to estimate the source signature. We briefly discuss the numerical model and show that the simulated signature is comparable to that predicted by *Nucleus* before demonstrating how the simulated source signature can be deconvolved from the observed data in order to improve the quality of the observations.

MODEL

We model the airgun dynamics using a similar treatment to that outlined in the seminal paper by Ziolkowski (1970). We solve the compressible Euler equations in the water and evaluate the solution on the bubble wall to obtain the modified Herring equation (Herring, 1941; Cole, 1948; Vokurka, 1986),

$$R\ddot{R} + \frac{3}{2}\dot{R}^2 = \frac{p - p_\infty}{\rho_\infty} + \frac{R}{\rho_\infty c_\infty}\dot{p} - \alpha\dot{R}, \tag{1}$$

where R and $\dot{R} = dR/dt$ are the radius and velocity of the bubble wall, respectively, p is the pressure inside the bubble, and p_∞, ρ_∞ and c_∞ are the pressure, density, and speed of sound, respectively, in the water infinitely far from the bubble. Numerical models of airgun signatures typically under-predict the damping observed in the data. Hence, α is included as a damping constant (Langhammer and Landrø, 1996) to obtain a better fit between simulation and observations.

The pressure perturbation in the water is related to the bubble dynamics by (Keller and Kolodner, 1956)

$$\Delta p(r,t) = \rho_\infty \left[\frac{\ddot{V}(t - r/c_\infty)}{4\pi r} - \frac{\dot{V}(t - r/c_\infty)^2}{32\pi^2 r^4} \right], \tag{2}$$

where Δp is the pressure perturbation in the water, r is the distance from the center of the bubble and $V = 4/3\pi R^3$ is the volume of the bubble. For further details on the numerical model the reader is referred to Watson et al. (2016) and the references therein.

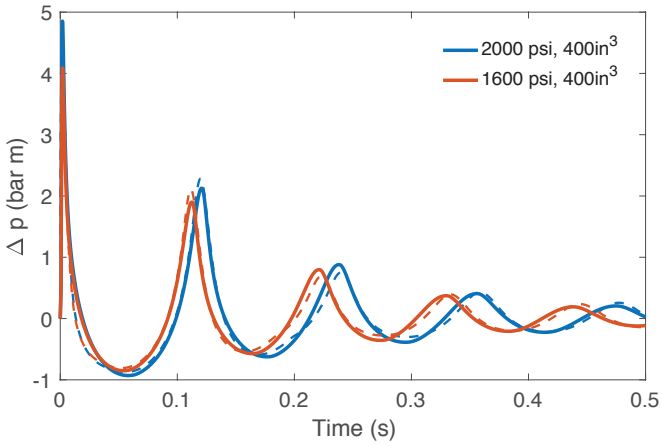

(a)

Figure 1: Our simulated signatures (solid) are in good agreement with the *Nucleus* signatures (dashed). [**CR**]

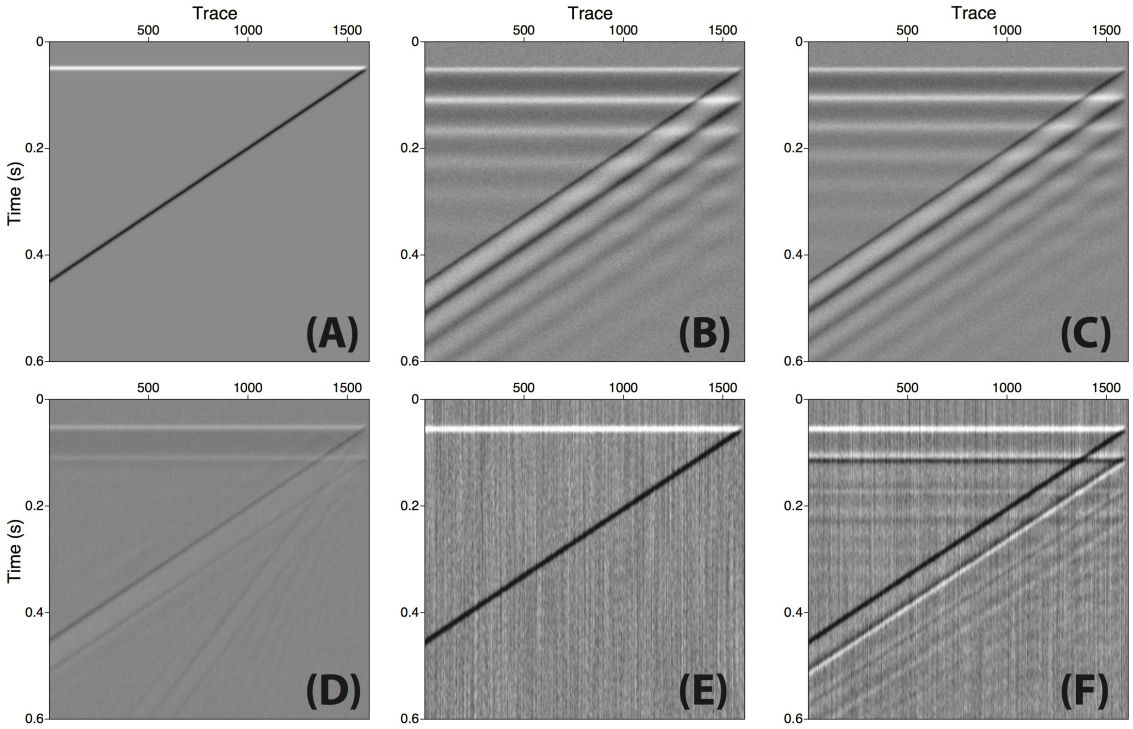

(a)

Figure 2: (A) Reflectivity model. (B) Synthetic data generated by convolving the reflectivity model with the simulated signature of the 2000 psi airgun shown in Figure 1.(C) Synthetic data generated by convolving the reflectivity model with the simulated signature of the 1600 psi airgun shown in Figure 1. (D) Prediction-error filter applied to the synthetic data shown in (B). (E) Synthetic data shown in (B) deconvolved with the correct signature (2000 psi airgun). (F) Synthetic data shown in (C) deconvolved with the wrong signature (2000 psi airgun). [**ER**]

SYNTHETICS

We illustrate the importance of using the correct signature in the designature process with a synthetic model of the subsurface consisting of a wedge of high acoustic impedance within a background medium with a lower acoustic impedance. There is a flat negative reflector at the top of the wedge and a dipping positive reflector at the base (Figure 2A).

Synthetic data are generated by convolving the reflectivity model with the two simulated signatures shown in Figure 1: a 400 in^3 airgun pressurized to 2000 psi (Figure 2B) and a 400 in^3 airgun that has developed an air leak and is pressurized to 1600 psi (Figure 2C). Random noise is added to give a signal-to-noise ratio of 2.

Figure 2E shows the reflectivity model produced when the synthetic data are deconvolved with the correct source signature. The result, as expected, is, apart from the addition of random noise, the same as the initial reflectivity model. Figure 2F shows the reflectivity model produced when the synthetic data are deconvolved with the wrong source signature. Here synthetic data were generated with the 1600 psi airgun signature but the deconvolution was performed with the 2000 psi airgun signature. The reflectivity model still contains significant ringing. Figure 2F illustrates the challenges faced in designaturing field data where the source signature may be unknown or may differ from what are expected. This underscores the importance of deconvolving with the correct source signature as well as the significance of having a source signature estimate when working with real data. This can be obtained by modeling or from direct measurements, such as with a near-field hydrophone.

Prediction-error filters (PFEs) are used to remove predictable information from a dataset. Figure 2D shows the application of a PEF to the synthetic data shown in Figure 2B. The PEF removes some of the ringing but introduces additional artificial noise. This is because the synthetic data involves two reflectors with different dips which introduces non-stationarity. As we estimate a single prediction-error filter for each trace, we cannot properly account for this non-stationarity which prevents the prediction-error filter from fully predicting all of the ringing and leads to additional artifacts.

DATA

The Apache Forties oil field data were acquired as part of an ocean-bottom node survey around three production rigs in the North Sea. The goal of the survey was to image gas clouds and other shallow drilling hazards near the rigs (Alves, 2015; Jennings and Ronen, 2016). We focus on the data collected around the Delta platform. The survey consisted of 14485 shots and 48 nodes. The source vessel circled the platform and spiraled inwards. Receivers were arranged in a roughly hexagonal pattern around the platform with a 50 m node spacing (Alves, 2015). The parabolic reflectors seen in the data in the time domain and the clear vertical bands of increased

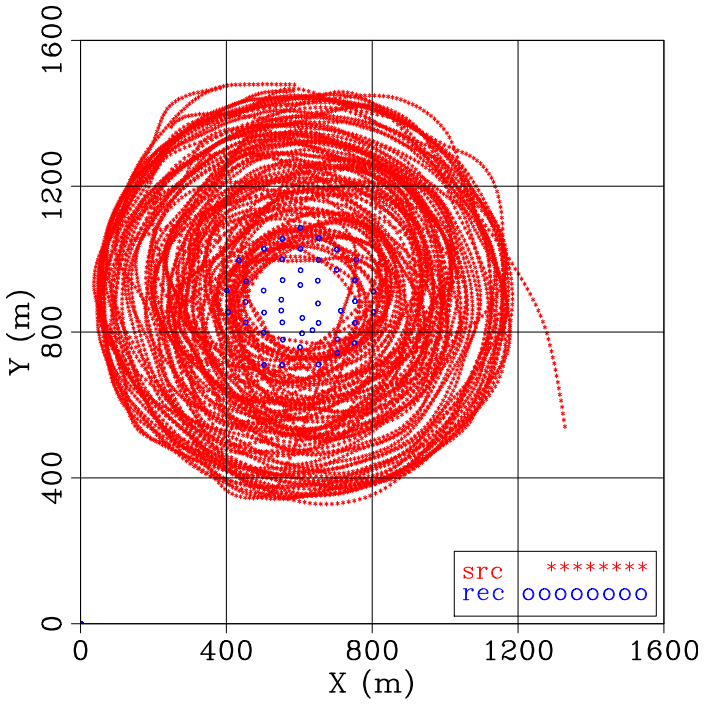

(a)

Figure 3: Shot-receiver geometry for the Apache Forties survey around the Delta platform. [**ER**]

energy in the frequency domain are a result of the spiral acquisition geometry. The horizontal banding is a result of the non-impulsive source signature.

The seismic source was a cluster of three 250 in^3 airguns. There were issues with the airgun array during acquisition. A leak developed around trace 7000 and the array operated with reduced pressure to at least one of the guns. Eventually, one gun failed, approximately at trace 9300 reducing the array to two 250 in^3 airguns. The changing source signature is clearly visible in the data shown in Figure 4. Once the air leak develops the dominant frequency of the source shifts to higher frequencies because less mass is ejected from the array into the water. This means that the bubble generated is smaller and hence oscillates faster. For analysis, we divide the data into three zones as shown in Figure 4.

The source signature is simulated in each of the three zones. A heuristic approach is taken to estimate the source signature for the array of airguns from the single airgun model described above. Initially the airguns do not interact. Therefore, the first instances of the signal are the summation of the pressure perturbations from the multiple airguns. Based on the detailed calculations of Barker and Landrø (2014), we introduce a scaling factor were the amplitude of the summation is reduced by 10%. By the time of the first bubble peak the bubbles from the multiple airguns have coalesced (the distance between the airguns is 1 m) and subsequently behave as a single large bubble. This can be simulated as a single airgun with a volume equal to

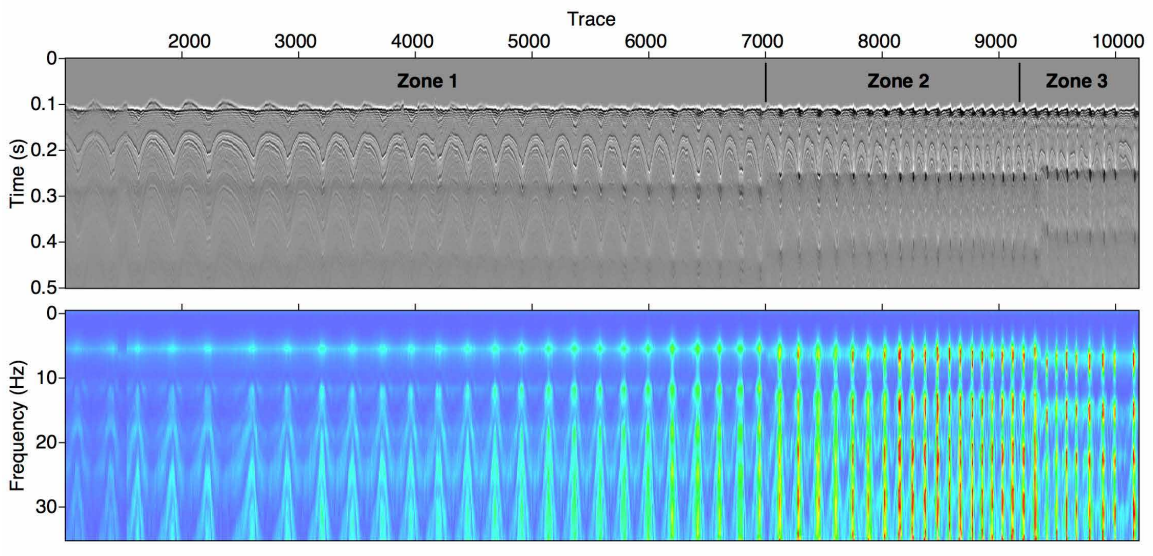

(a)

Figure 4: Data in the time (top) and frequency (bottom) domain. Note the discontinuities around trace 7000 and trace 9300 due to the airgun failure. [**ER**]

the total volume of the array. The signal is tapered between these two limits to give a smooth source signature. Note that this approximation can be justified for a small array of closely spaced airguns. This approach is not valid for larger arrays where directivity effects become important and bubble coalescence is more complicated.

Figure 5 shows the deconvolution of the data using the simulated signatures (5A and 5B) and using a prediction-error filter (5C). Figure 5A is designatured using a different simulated signature for each of the three zones. Figure 5B is designatured using the simulated signature from zone 1. The results are the same for zone 1. For zones 2 and 3 bubble energy remains in Figure 5B that is not present in Figure 5A. As with the synthetics, this demonstrates the importance of deconvolving with the correct source signature.

Note that for both Figure 5A and Figure 5B a dark band of energy around 0.25 s remains after designaturing. The energy increasing to the right in each zone. This may be due to the source signature changing within each zone or may be an artifact of the spiral acquisition geometry.

CONCLUSION

We show how deterministic modeling of the airgun signature can be used to designature ocean bottom node data. We show that using an incorrect signature, such as not accounting for a pressure drop due to an air leak, may do more harm than good. We also show that using nondeterministic prediction error filter may create spurious

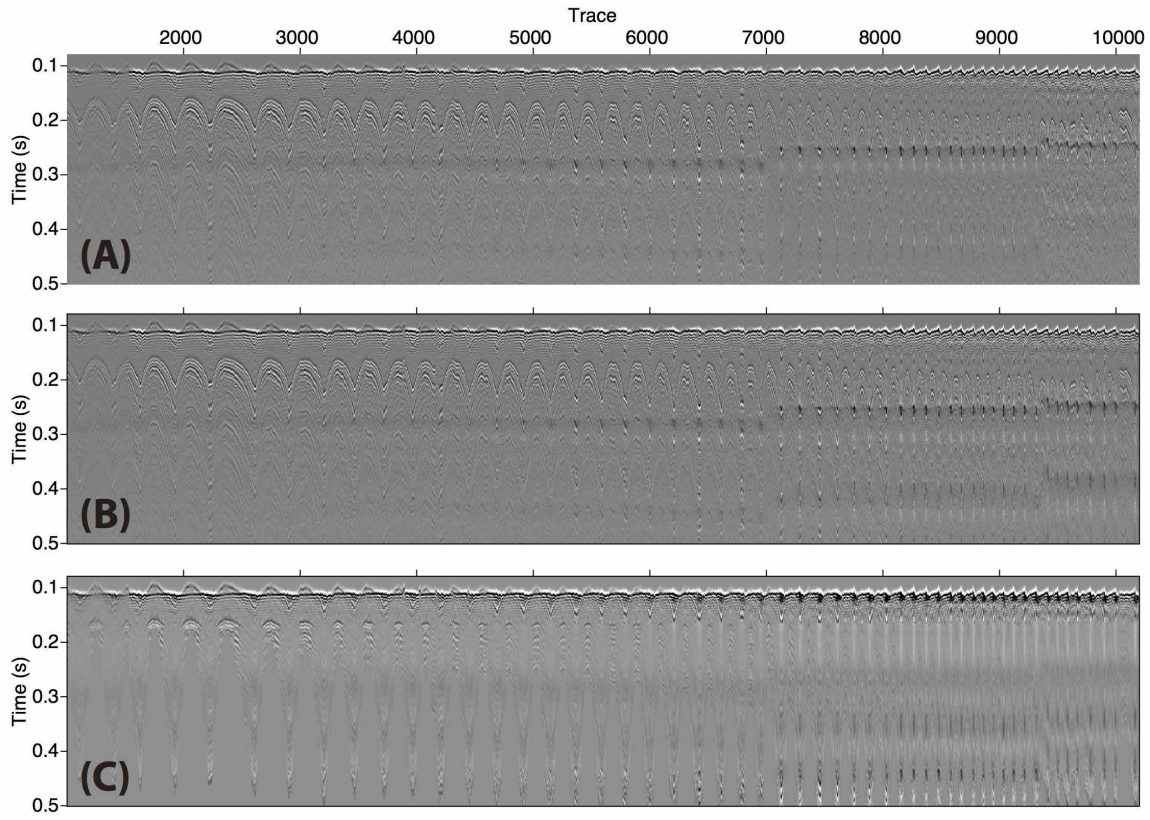

(a)

Figure 5: (A) Data deconvolved using the simulated source signature. The source signature is simulated for each of the three zones. (B) Data deconvolved using the simulated source signature from zone 1 to deconvolve from all three zones. (C) Data deconvolved using a prediction-error filter. The prediction error filter is applied zone by zone. [**ER**]

events.

ACKNOWLEDGEMENTS

We thank Apache North Sea Limited for access to the data set and permission to publish. We acknowledge the Stanford Exploration Project and their sponsors for financial support.

REFERENCES

Alves, G., 2015, Overview of the Apache Forties data set: SEP-Report, **160**.

Barker, D. and M. Landrø, 2014, An alternative method for modeling close-range interactions between air guns: Geophysics, **79**, P1–P7.

Cole, R. H., 1948, Underwater explosions: Princeton University Press.

de Graaf, K. L., I. Penesis, and P. A. Brandner, 2014, Modelling of seismic airgun bubble dynamics and pressure field using the Gilmore equation with additional damping factors: Ocean Engineering, **76**, 32–39.

Dragoset, B., 2000, Introduction to air guns and air-gun arrays: The Leading Edge, **19**, 892.

Herring, C., 1941, Theory of the pulsations of the gas bubble produced by an underwater explosions: Technical report, Office of Scientific Research and Development.

Jennings, J. and S. Ronen, 2016, Separation of simultaneous source blended data using radiality and source similarity attributes: SEP-Report, **163**.

Keller, J. B. and I. I. Kolodner, 1956, Damping of underwater explosion bubble oscillations: Journal of Applied Physics, **27**, 1152–1161.

Kryvohuz, M. and X. Campman, 2016, Optimization of sea surface reflection coefficient and source geometry in conventional dual source flip/flop marine seismic acquisition: SEG Annual Meeting, Dallas, Texas, 188–192.

Landrø, M. and R. Sollie, 1992, Source signature determination by inversion: Geophysics, **57**, 1633–1640.

Landrø, M., S. Strandenes, and S. Vaage, 1991, Use of near-field measurements to compute far-field marine source signatures: evaluation of the method: First Break, **9**, 375–385.

Langhammer, J. and M. Landrø, 1996, High-speed photography of the bubble generated by an airgun: Geophysical Prospecting, 153–173.

Laws, R., M. Landrø, and L. Amundsen, 1998, An experimental comparison of three direct methods of marine source signature estimation: Geophysical Prospecting, **46**, 353–389.

Li, G. F., M. Q. Cao, H. L. Chen, and C. Z. Ni, 2010, Modeling air gun signatures in marine seismic exploration considering multiple physical factors: Applied Geophysics, **7**, 158–165.

Vokurka, K., 1986, Comparison of Rayleigh's , Herring's , and Gilmore's Models of Gas Bubbles: Acta Acustica united with Acustica, **59**, 214–219.

Watson, L. M., E. M. Dunham, and S. Ronen, 2016, Numerical modeling of seismic airguns and low-pressure sources: SEG Annual Meeting, Dallas, Texas, 219–224.

Yilmaz, Ö., 2011, Seismic data analysis: Processing, inversion, and interpretation of seismic data: Society of Exploration Geophysicists.

Ziolkowski, A., 1970, A Method for Calculating the Output Pressure Waveform from an Air Gun: Geophysical Journal International, **21**, 137–161.

———, 1991, Why dont we measure seismic signatures?: Geophysics, **56**, 190–201.

Ziolkowski, A. M., G. E. Parkes, L. Hatton, and T. Haugland, 1981, British patent appl. no. 8 116 527.

———, 1984, U.S. patent no. 4,476,553.